# Field and Chirality Effects on Electrochemical Charge Transfer Rates: Spin Dependent Electrochemistry

**Prakash Chandra Mondal,[†] Claudio Fontanesi,[†,‡] David H. Waldeck,[§] and Ron Naaman[*,†]**

[†]Department of Chemical Physics, Weizmann Institute of Science, Rehovot 76100, Israel, [‡]Department of Chemical and Geological Science, University of Modena and Reggio Emilia, Via G. Campi 183, 41125 Modena, Italy, and [§]Department of Chemistry, Pittsburgh University, Pittsburgh Pennsylvania 15260, United States

**ABSTRACT** This work examines whether electrochemical redox reactions are sensitive to the electron spin orientation by examining the effects of magnetic field and molecular chirality on the charge transfer process. The working electrode is either a ferromagnetic nickel film or a nickel film that is coated with an ultrathin (5−30 nm) gold overlayer. The electrode is coated with a self-assembled monolayer that immobilizes a redox couple containing chiral molecular units, either the redox active dye toluidine blue O with a chiral cysteine linking unit or cytochrome *c*. By varying the direction of magnetization of the nickel, toward or away from the adsorbed layer, we demonstrate that the electrochemical current depends on the orientation of the electrons' spin. In the case of cytochrome *c*, the spin selectivity of the reduction is extremely high, namely, the reduction occurs mainly with electrons having their spin-aligned antiparallel to their velocity.

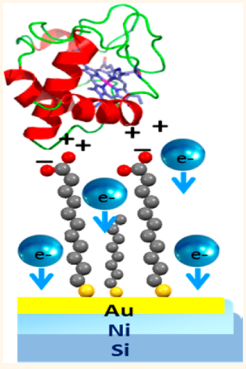


**KEYWORDS:** self-assembled monolayers · spin · chirality · cytochrome c · cysteine

For the past two decades, self-assembled monolayers (SAMs) have been used to manipulate the surface properties of electrodes and to explore how the charge transfer rates depend on features of the electrochemical interfaces.[1,2] These studies have encompassed a broad range of systems, from fundamental studies into the electrochemical kinetics of small molecules to studies that manipulate and control the redox exchange with biomolecules such as proteins and enzymes.[3] The present work uses self-assembled films of chiral molecules to explore whether the electrons' spin orientation affects electrochemical charge transfer processes, and then extends this approach to examine whether the charge transfer process in cytochrome *c* is affected by the spin orientation. Recent experimental and theoretical studies have revealed that the electron transmission through chiral molecules depends on the electrons' spin orientation, an effect referred to as Chiral Induced Spin Selectivity (CISS).[4,5] The studies described here use a chiral linker molecule between the redox moiety and a ferromagnetic electrode to provide a spin filter for the electrons, *via* the CISS effect, and they combine it with an externally applied static magnetic field that switches the direction of magnetization of the ferromagnetic electrode to unveil the spin selectivity in the electron transfer process.

Magnetic field effects on electrochemical processes have been known for decades and almost all of them are linked with transport of charge carriers in the electrolyte.[6−12] These magnetic field effects have been most often explained by the Lorentz force, which arises from the magnetic field acting on the freely moving charge carriers (electrons or ions),[13] or the Kelvin force, which arises from the gradient of the magnetic field acting on paramagnetic species in the electrochemical solution.[14,15] Magnetic field effects on redox process have been reported before in biorelated systems[16−19] and also specifically with cytochrome *c*.[20] Usually, they have been attributed to either the Lorenz or the Kelvin forces.

Although magnetic field effects on the electron transfer kinetics of radical pairs have been well studied,[21−23] the investigation

* Address correspondence to ron.naaman@weizmann.ac.il.

Received for review February 5, 2015 and accepted March 9, 2015.

**Published online March 09, 2015**
**10.1021/acsnano.5b00832**

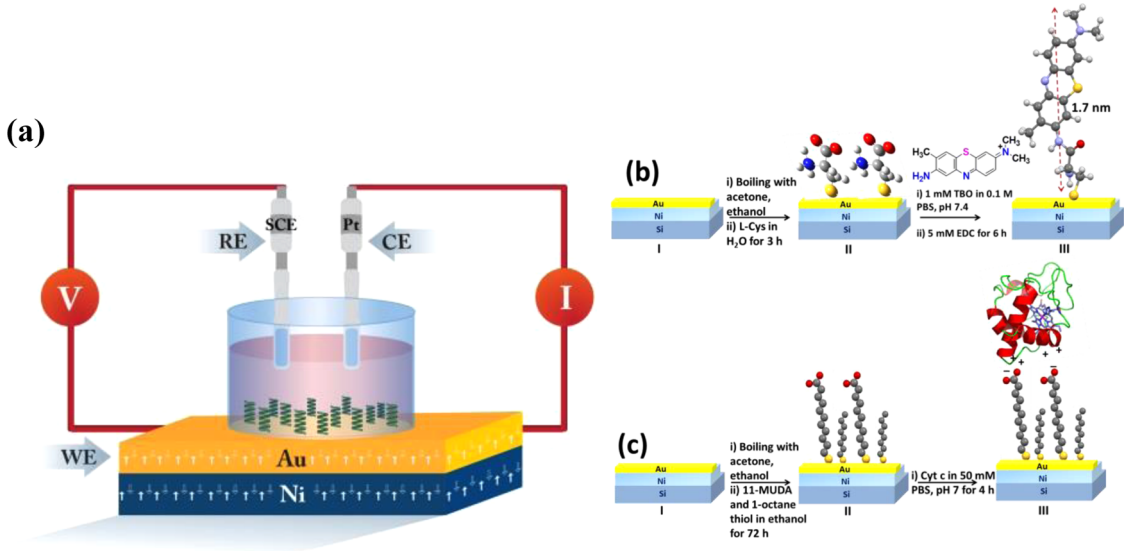


**Figure 1. Panel (a) shows a schematic diagram that illustrates the electrochemistry setup, in which a gold-coated Ni film is the working electrode (WE), a platinum wire is the counter electrode (CE), and a Saturated Calomel Electrode (SCE) is the reference (RE) electrode. The Ni electrode is magnetized with an external magnetic field (H) that is applied by placing a permanent magnet below the Ni electrode, with its magnetic dipole pointing up or down (white and yellow arrows, respectively). Panel (b) illustrates the protocol for covalently tethering TBO to the working electrode *via* a cysteine (L or D) linker. Panel (c) illustrates the protocol for preparing a mixed monolayer of 11-mercaptoundecanoic acid and 1-octanethiol and immobilizing cytochrome *c* on it.**

of magnetic field effects on electrochemical rate constants is less explored.[24−27] In an early report, Lee *et al.*[25] investigated the electroless deposition of $Ni^{2+}$ to Ni metal as a function of the externally applied magnetic field; they identified a dependence which they interpreted as arising from changes in the kinetics of the $Ni^{+}$ radical intermediate. In other work, Devos *et al.*[27] examined redox kinetics for a number of different systems (diffusion controlled, kinetic controlled, and mixed) by electrochemical impedance spectroscopy and found that the kinetic parameters were insensitive to the applied field. More recently, Lyons *et al.*[28,29] investigated self-assembled monolayer films, which tethered the ferrocene/ferrocenium redox couple to a gold electrode, and observed that a 0.5 T static magnetic field, which was applied in a direction parallel to the electrode surface, introduced irreversibility into the faradaic peak of the voltammogram. Even though the redox moiety was surface immobilized, they concluded that the ion pairing kinetics with the ferrocenium was the rate-limiting step and controlled by counterion transport, which was affected by localized magneto-hydrodynamic stirring. In a different study, a magnetic field effect on the ferrocene redox couple was reported for the case where an external magnetic field was applied perpendicular to the surface of a ferrocene monolayer film. These observations were explained by a change in the tilt angle of the alkyl chains and a subsequent change in the dominant electron tunneling pathways through the film.[30]

In addition to fundamental studies of charge carrier transport, an applied external magnetic field has been shown to affect the morphology of electrodeposited films,[8] and in some cases lead to the creation of new electrode materials that display enantiomeric selectivity.[31,32] In related activities, workers have explored the development of chiral electrodes and chemically modified electrodes, in particular, for applied use in enantio-recognition.[33] Common approaches are the imprinting of chirality in a conductive polymer by a chiral molecule[34] or by adsorbing chiral molecules on the surface of the electrode.[35] None of these studies have examined whether the "chiral electrode" gives rise to spin selectivity in electron transfer, however.

To examine the spin selectivity of an electron transfer process, it is necessary to inject spin polarized electrons into the system. From research in spintronics,[36] it is known that applying a magnetic field to ferromagnetic electrode films can be used to eject preferentially one spin orientation from the electrode, and from research on the CISS effect,[4,5] it is known that chiral molecules can act as electron spin filters. This study analyzes the effect of spin on the charge transfer by observing how the magnetic field selection and the chiral molecule filtering interact and affect the electrochemical current. This work coats a magnetized electrode with chiral molecules containing a redox moiety and investigates how the electron transfer reaction depends on the chirality and the magnetization direction. The experimental setup is shown schematically in Figure 1a. It consists of a nickel, or gold-coated-nickel, working electrode that is chemically modified with a self-assembled monolayer (SAM) of chiral molecules. An external magnetic field is applied with a permanent magnet that is underneath the nickel working electrode and its field direction is changed by physically

rotating the magnet by 180°. In this arrangement, the nickel working electrode can be magnetized so that its magnetic dipole is pointing toward the solution or away from it (UP or DOWN, respectively).

While nickel has the advantage of being ferromagnetic and readily prepared as a film electrode, it is oxidized under aerobic conditions and in an electrochemical cell. Although a self-assembled monolayer coating can be used to inhibit the electrode corrosion, as well as to control the placement of the redox molecules, it is challenging to prepare the electrochemical cell with a Ni working electrode and ensure that oxidation is prevented. To overcome this challenge, the Ni electrode was protected by an ultrathin Au overlayer (ranging from 5 to 30 nm) upon which the redox molecules are adsorbed. Indeed, while it was almost impossible to have undenaturated cytochrome *c* on the bare Ni electrode, when coated with gold the cytochrome *c* was found to be stable and possess a redox potential that is consistent with that for cytochrome *c* adsorbed on gold. Although the Au layer enhances the chemical stability of the metal electrode, its large spin−orbit coupling reduces the spin polarization of the injected electrons. Thus, the dependence of the spin polarized current on the Au film thickness was quantified also.

In the present study, the magnetic field effect on the electrochemistry is explored for two different cases. In the first case, the redox active dye toluidine blue O (TBO) is covalently attached to a cysteine group (either L or D) which binds to the electrode surface; thus, the molecules are adsorbed as a self-assembled monolayer on the nickel/gold surface; see the schematic illustration in Figure 1b. The second case uses the globular redox protein cytochrome *c* which is adsorbed on the working electrode through electrostatic interactions with a mixed monolayer film of 11-mercaptoundecanoic acid and 1-octanethiol; see the schematic in Figure 1c. (see Experimental Section). The monolayer films were characterized by IR, AFM, and contact angle measurements, and the chirality of the L/D-cysteine films was verified by enantioselective cyclic voltammetry measurements using a chiral redox couple (see Figures S1−S5, Table S1 in Supporting Information).

## RESULTS AND DISCUSSION

**Voltammetry of TBO Monolayers.** Figure 2 shows cyclic voltammograms that were collected on Ni electrodes coated with a 10 nm thick Au film. Panel A shows the voltammograms obtained for a D-cysteine linked TBO (D-Cys-TBO) redox group as a function of the magnetic field direction. Note that the faradaic current is higher for the case in which the magnetic field is oriented away from the monolayer/solution interface ("DOWN"). The only feature of the experimental setup that is changed between the two measurements is the magnet; the electrode and all other features of the setup

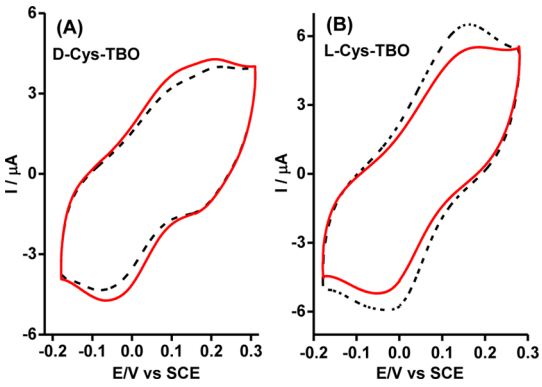


**Figure 2. Cyclic voltammograms are shown for D-cysteine-TBO (panel A) and L-cysteine-TBO (panel B) self-assembled monolayers on a 200 nm nickel/10 nm gold metal film electrode. When the nickel is magnetized, it is either with its magnetic moment pointing UP, toward the monolayer (dashed black curve), or DOWN, away from the monolayer (solid red curve). Voltammograms were recorded in 0.1 M PBS of pH 7.4 containing 10 mM KCl as supporting electrolyte at 50 mV $s^{-1}$.**

remain unchanged. Panel B shows data for L-cysteine linked TBO (L-Cys-TBO) in which the faradaic current is higher for the case where the magnetic field is oriented toward the monolayer/solution interface ("UP"). Thus, the magnetic field dependence is of opposite sign for the two different chiralities of the cysteine. Note that it is not possible to compare the absolute signal levels between the data in panels A and B, because the coverage of TBO, as well as other details of the working electrode preparation, can change. The main result of these measurements is that the sign of the asymmetry is inverted when the chirality of the SAM is inverted. These data reveal that the electrochemical current depends on both the chirality of the cysteine linker and the magnetic field direction. This dependence cannot be explained by a magneto-hydrodynamic effect because the transport in the electrolyte should not depend on the film chirality or on whether the magnetic field direction is UP or DOWN, *i.e.*, whether the north or south pole is nearer to the electrode and normal to its surface. The observations can be explained using the chiral induced spin selectivity (CISS) effect, however.[4,5,37]

To quantify the asymmetry in the current, we define the spin polarization (SP) as

$$\mathrm{SP} = \frac{I(V)_{\uparrow} - I(V)_{\downarrow}}{I(V)_{\uparrow} + I(V)_{\downarrow}} \times 100\%$$

in which $I(V)_{\uparrow}$ is the voltage dependent current when the magnetic field is pointing UP and $I(V)_{\downarrow}$ is the voltage dependent current when the magnet field is pointing DOWN. If we select the peak potential of the current as the place to evaluate SP, we find a value of $+9 \pm 1\%$ for the L-Cys-TBO film in the forward sweep (at +160 mV) and $-7.5 \pm 0.5\%$ for the reverse sweep (at −24 mV). For the D-Cys-TBO film, we find an SP of $-6 \pm 1\%$ for the forward sweep (at +185 mV) and $+4.7 \pm 0.5\%$ for the

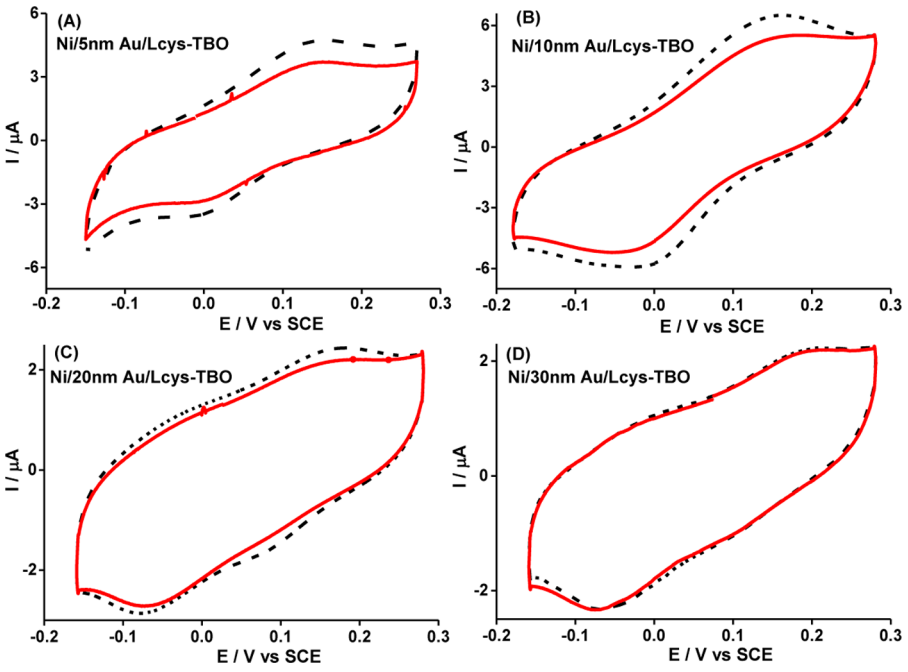


**Figure 3. Voltammograms are shown for L-Cys-TBO monolayers adsorbed on gold-coated Ni electrodes for four different thicknesses of the gold film overlayer (panels A, B, C, and D represent 5, 10, 20, and 30 nm thick layers, respectively). The curves were obtained when the nickel is magnetized either with its magnetic moment pointing UP, toward the monolayer (dashed black curve), or DOWN, away from the monolayer (solid red curve). Voltammograms were recorded in a 0.1 M PBS buffer (pH 7.4) containing 10 mM KCl.**

reverse sweep (at −56 mV). Note that the waveform in the forward sweep D-Cys-TBO is suggestive of a second peak, and this is attributed to the limited enantiomeric purity of the D-cysteine used to make the D-Cys-TBO.[38] This limited purity may also explain the differences in the magnitude of the spin polarization between the two enantiomers. A control experiment, in which the gold-coated nickel electrode (10 nm Au/Ni) was coated with the redox active achiral 6-(ferrocenyl)hexanethiol monolayer (see PMIRRAS data in Supporting Information Figure S6) showed no significant magnetic field effect, < 1% (see Figure S7 in the Supporting Information ). Because TBO is very sensitive to the electrolyte,[39] the electrolyte could not be changed for control studies.

Because of the strong spin−orbit coupling, the Au overlayer film can depolarize the electron current. This effect was studied by changing the Au overlayer thickness. It is important to realize that the role of the gold in stabilizing the electrode was verified by observing reproducible signals as a function of time, while with uncoated nickel electrodes, the signal deteriorated with time. Figure 3 shows voltammograms that were obtained for L-Cys-TBO monolayers on gold-coated Ni electrodes with four different Au layer thicknesses, ranging from 5 to 30 nm (*i.e.*, 5, 10, 20, and 30 nm thick Au). AFM results reveal that a smooth coverage of gold on the nickel exists only when the gold layer thickness is 20 nm or more. However, also for thinner averaged thickness the nickel is coated with gold (see Figure S4 in Supporting Information). For each average thickness, the voltammogram is measured as a function of the magnetic field direction and it displays a positive SP; however, the value of the SP decreases systematically as the Au layer thickness increases. These observations support those shown in Figure 2 and confirm that the asymmetry in the current (SP value) arises from electron current at the metal electrode/monolayer interface, rather than ion currents or ion pairing effects at the monolayer/solution interface.

Figure 4 presents data on the spin dependent voltammetry for different thicknesses of the Au overlayer. Panel A shows a plot of the spin polarization as a function of Au thickness. These SP values were obtained from the peak current in the forward sweep of the voltammograms shown in Figure 3. The SP is about 11% for a 5 nm thick gold layer and it decreases monotonically as the layer thickness increases, reaching zero for layers thicker than 30 nm; *i.e.*, pure Au shows 0% SP. Note that when the thickness is extrapolated to zero, the polarization exceeds 14%, even though the chiral molecule is small and has no secondary helical structure. Previous work shows that the spin polarization of electrons ejected from Ni depends on the conditions (crystallinity, temperature, *etc.*), but never exceeds about 40%.[40,41] To estimate a bound for the spin filtering by the chiral molecules, assume that the polarized electrons from the Ni is 40%, then the actual spin polarization of electrons transmitted through cysteine is on the order of 30% or higher.

In addition to changes in the peak current and its asymmetry in the magnetic field, the oxidation potential increases with increasing thickness of the gold

film (Figure 4B). In the approximation of no junction potential at the Ni/Au interface, a peak potential shift could arise if the electron transfer rate was changed by the thickness of the Au overlayer. For a given scan rate (10 mV $s^{-1}$), an anodic shift of the peak potential value corresponds to a slowing of the electron transfer rate. When attempting to measure a voltammogram at higher scan rates (>50 mV $s^{-1}$), no signal was observed, supporting a slow electron transfer process. This interpretation may reflect a dependence of the electron transfer rate on the spin polarization; *i.e.*, the more polarized current (thinner Au layer) has a faster electron transfer rate (smaller peak shift) through the chiral molecules. Alternatively, the difference in rate constant may reflect a dependence on any potential drop at the Ni/Au interface.

**Electrochemistry of Immobilized Cytochrome *c*.** To explore whether the spin preference could be manifested in electron transfer with a redox protein, we investigated the oxidation/reduction of the globular protein cytochrome *c*. Mixed monolayer films of 11-mercaptoundecanoic acid and 1-octanethiol were prepared on gold-coated nickel electrodes (a nickel electrode coated with a 10 nm gold layer) and cytochrome *c* was bound electrostatically to the electrode surface. These films were characterized by polarization modulated infrared reflection absorption spectroscopy (PMIRRAS) measurements (see Figure S2 in Supporting Information). These assemblies were studied by cyclic voltammetry and chronoamperometry.

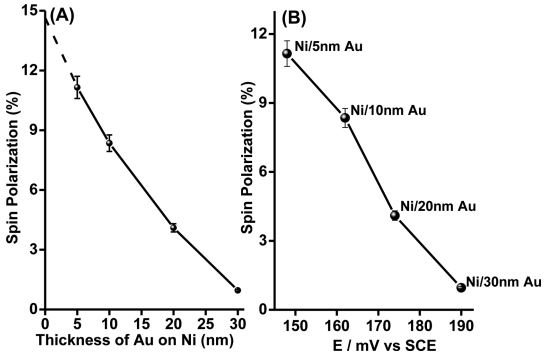


**Figure 4. Panel A shows a plot of the spin polarization *versus* the thickness of the gold layer for the redox reaction of TBO attached by cysteine to the electrode (data taken from Figure 3). The spin polarization was calculated from the current at the peak potential of the corresponding oxidation wave, which is plotted in panel B as a function of Au film thickness.**

Figure 5A shows cyclic voltammograms for the adsorbed films of cytochrome *c* for two different magnetic field directions (UP and DOWN). In this case, the cytochrome *c* displays a stable electrochemical response with an oxidation and reduction potential at +0.21 and +0.13 (with half-wave redox potential, $E_{1/2}$ at +0.17 V), respectively *versus* SCE; see Figure 5A. This redox potential is in good agreement with earlier work.[42] While the potential does not depend on the magnetic field direction, the magnitudes of the current peak in the two voltammograms show a dependence on the magnetic field direction. In contrast to the L-Cys-TBO case, these data display a higher current when the magnetic field is oriented DOWN than when it is oriented UP. This finding indicates that the preferred spin orientation is antiparallel to the electrons' direction of propagation (Figure 5). The SP measured at 0.13 or at 0.19 V is −11 ± 2%. As a control experiment, the protein was denatured by applying a voltage of −1.0 V, which is negative enough to denature the protein but not strip it or the self-assembled monolayer film from the electrode (see Figure S8 in Supporting

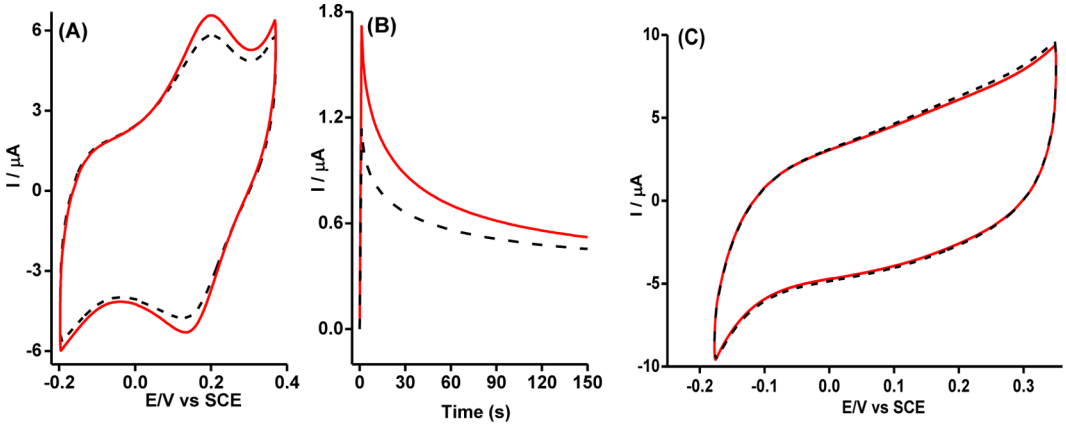


**Figure 5. (A) Voltammograms are shown for cytochrome *c* immobilized on a mixed monolayer of 11-mercaptoundecanoic acid and 1-octanethiol that is chemically adsorbed on a 10 nm thick gold film on top of nickel. The measurements were carried out in a 50 mM phosphate buffer solution of pH 7 at a scan rate of 50 mV $s^{-1}$. The black dashed curve and the red solid curve correspond to a magnetic field pointing UP and DOWN, respectively. (B) The image shows current−time plots from chronoamperometry measurements on a nickel/gold electrode that is coated with a mixed SAM of methyl-terminated and carboxylic acid terminated thiols on which cytochrome *c* was immobilized electrostatically. The measurements were performed at 0.25 V (vs SCE) in 50 mM phosphate buffer solution of pH 7. (C) The voltammograms obtained after applying −1 V on the adsorbed cytochrome *c*, that causes it to denature. The solid red curve corresponds to a magnet aligned antiparallel to the surface normal, while the dashed black curve corresponds to a magnetic field aligned parallel to the surface normal.**

Information). In this case, the faradaic peak is lost and no difference in the current is observed for the two magnetic field directions (see Figure 5C). We assume that upon applying such a high voltage, the structure and charge distribution in the polypeptide backbone is changing, and the denatured form is not functioning as a spin filter. This effect of change in structure/charge distribution on the spin filter was also observed when bacteriorhodopsin was excited by light.[43] The observed spin filtering in the small cysteine molecule and its disappearance upon denaturation of the cytochrome *c* suggests that indeed the spin filtering is not only a matter of chirality but it depends also on the charge distribution. It has been observed before that when the dipole moment of a molecule is very small, no spin filtering is observed even if the system is chiral (*vide infra*).[44]

Comparing the SP in cytochrome *c versus* that of cysteine-TBO, both obtained from the voltammetry on a Ni electrode with a 10 nm thick gold overlayer, one finds that the SP for cytochrome *c* is larger by about 30%. Given that the corrected SP in cysteine (after considering the spin depolarization by the gold and the spin polarization in Ni) is 30−40% (*vide supra*), a comparison indicates that the SP is on the order of 40−70% for cytochrome *c*. If one considers the SP based on the chronoamperometry measurements, then the spin selectivity of the redox process in cytochrome *c* is even higher.

The reversed spin filtering observed in cytochrome *c*, as compared to cysteine-TBO, results from the sensitivity of the filtering to the direction of the electric field applied on the moving electron. The spin orbit coupling term includes the expression $\vec{v} \times \vec{E}$, in which $\vec{v}$ is the electron's velocity and $\vec{E}$ is the electric field. This field is responsible to the effective spin orbit coupling and it depends on the handedness of the system and on the gradient of the electric potential.[5,44] Hence upon changing sign of the field, or in other words, the direction of the gradient of the electrostatic potential, the preferred spin for the electron transfer changes. This effect was observed before when the preferred spin in transmission was found to be the opposite in DNA *versus* oligopeptides.[45] It is important to realize that this model is consistent with the relative magnitudes of the cathodic and anodic (reduction and oxidation) waves in the voltammetry. The preferred spin of the electrons in the two processes are aligned in the opposite direction. However, while in the case of the reduction, electrons are injected from the majority spin states of the magnetized Ni, in the oxidation stage, they are injected into the minority spin states. The majority and minority states relate to opposite spin alignment for a given magnetization.

## CONCLUSIONS

This study used an external magnetic field and chiral redox couples to probe the spin dependence of oxidation and reduction for the redox dye molecule TBO and the protein cytochrome *c*. A spin-polarized current was injected using a ferromagnetic nickel working electrode, which was subject to an external magnetic field. Because of the chemical instability of the nickel surface, it was coated with an ultrathin overlayer of gold, which is commonly used in the study of adsorbed molecules. To investigate the importance of spin depolarization by the large spin orbit coupling of gold, voltammetry studies were performed for different thicknesses of the Au overlayer and it was found that significant spin polarization is maintained up to a thickness of about 20 nm. This gold-coating method enabled the study of spin selectivity for the protein cytochrome *c*, and it was found to display an extremely high spin selectivity for the redox process.

## EXPERIMENTAL SECTION

**Materials.** Toluidine blue O (TBO), 1-ethyl-3-(3-(dimethylamino)propyl)-carbodiimide (EDC), 1-octanethiol, 11-mercapto undecanoic acid (MUDA), L- and D-cysteine, *R* and *S*−*N*,*N*-dimethyl-1-ferrocenylethylamine, $K_4Fe(CN)_6$, $K_3Fe(CN)_6$, tetrabutylammonium tetrafluoroborate (TBATFB), 6-(ferrocenyl)-hexanethiol and KCl were purchased from Sigma-Aldrich and used without further purification. Cytochrome *c* (Sigma C 7752, from horse heart) was stored at −4 °C before use. Solvents (AR grade) were purchased from Merck and used as received. Single crystal silicon ⟨100⟩ (400 Ω/cm$^2$) of 525 ± 25 $\mu$m thickness (300 nm of thermal oxide on the surface) was purchased from University Wafers, Inc. All metals (Ni, Au, Ti) used during evaporation were purchased from Kurt J. Lesker.

**Electrochemical Measurement.** Cyclic voltammetry (CV) and chronoamperometric measurements were performed using a Bio-Logic potentiostat SAS (Model SP-200) with EC Lab software (V 10.36). Voltammetry measurements were performed in a standard three electrode electrochemical cell configuration. A scheme of the working electrode design is presented in Figure 1a. A permanent magnet of magnetic field 0.5 T was placed directly behind the 0.5 mm thick silicon substrate that supported the 200 nm thick working electrode which consisted of a nickel film or a nickel film coated with an ultrathin (5−30 nm) layer of gold. The chronoamperometric measurements for immobilized cytochrome *c* were performed at 0.25 V (vs SCE) in 50 mM phosphate buffer solution of pH 7. The counter electrode was platinum and the reference electrode used was KCl-saturated calomel. Spin dependent electrochemical measurements were performed at room temperature. Details on the evaporation and characterization of the films are given in the Supporting Information.

Two types of molecules were investigated. The first was either L- or D-cysteine to which TBO was covalently attached as the redox species. The molecules were adsorbed as self-assembled monolayers on gold coated nickel, as shown schematically in Figure 1b,c. The second redox molecules adsorbed were cytochrome *c* through electrostatic interaction with a mixed monolayer of 11-mercaptoundecanoic acid and 1-octanethiol. Supporting Information Figure S2 presents the IR spectra of the adsorbed layers.

**Preparation of Monolayers.** Freshly prepared Ni substrates coated with Au (5−30 nm) were properly cleaned in hot

acetone, followed by ethanol for 15 min each, and then dried gently under Ar. The gold coated substrates were then plasma cleaned in oxygen (at ~0.4 Torr) for 1 min. Subsequently, the substrates were immediately immersed into a 10 mM solution of cysteine (L or D) in deionized water (18.2 MΩ·cm at 25 °C) for 3 h at room temperature. The modified substrates were thoroughly rinsed with water and subsequently dried in a stream of argon and used immediately afterward for characterization. The cysteine modified substrates were allowed to react with 1 mM TBO in 0.1 M potassium phosphate buffer solution (PBS) of pH 7.4 in the presence of 5 mM EDC for 6 h. The substrates were washed with a 0.1 M PBS solution and dried under a stream of Ar.

**Electrostatic Interaction with a Mixed Monolayer.** The 10 nm gold coated nickel electrodes were chemically modified by immersion of the substrates into an ethanol solution containing 1 mM of 11-mercaptoundecanoic acid and 1-octanethiol (1:9, mole ratio) for 72 h to form the mixed monolayer. The modified electrode was rinsed with ethanol and then dried under an Ar stream. Subsequently, the substrates were dipped into a 50 mM PBS of pH 7 for 30 min under an Ar atmosphere. The electrodes were immersed in a 50 $\mu$M cytochrome *c* solution (see UV−vis spectra of the cyt *c* in Supporting Information Figure S9) in 50 mM PBS of pH 7 (purged with argon gas) for 4 h at 4 °C under Ar in order to electrostatically bind the cytochrome with −COOH terminated mixed SAM. The cytochrome *c*/mixed SAM/electrode assemblies were rinsed with the same buffer solution before performing electrochemical measurements. 6-(Ferrocenyl)hexanethiol monolayer was prepared in similar way (see PMIRRAS data in Supporting Information Figure S6).

**Evaluating the Spin Polarization.** In all of the experiments, the magnetic field is applied along the axis normal to the Ni electrode surface. By controlling the direction of the applied magnetic field (parallel or antiparallel to the electrode axis), it is possible to inject electrons that have mainly one spin orientation or the other. The spin polarization was confirmed by monitoring the asymmetry in the faradaic current peak of the cyclic voltammograms and by observing the asymmetry in the current−time profiles that are measured by chronoamperometry. The chronoamperometry data show that the asymmetry in the current response is highest just after the potential jump is applied, and it decreases with time as the double layer forms.[46,47]

The dye molecule, toluidine blue O (TBO) was tethered to the working electrode through either an L- or D-cysteine linkage. The molecules were adsorbed as self-assembled monolayers on gold coated nickel, as shown schematically in Figure 1A, and cyclic voltammograms were measured as a function of (i) magnetic field direction, (ii) cysteine chirality, and (iii) thickness of the Au layer. Voltammetry experiments were performed to confirm that the current increases linearly with the scan rate and the peak potential of the faradaic current changes systematically. These data are reported in the Supporting Information (see Figures S10 and S11) and show the confinement of the redox molecules on the surfaces.

*Conflict of Interest:* The authors declare no competing financial interest.

*Acknowledgment.* Dr. Kiran Vankay and Dr. Sidney Cohen are acknowledged for performing the AFM studies. The research was supported by an ERC-Adv grant and by the Israel Ministry of Science. D.H.W acknowledges support from the NSF (DMR-1412030).

*Supporting Information Available:* PMIRRAS of monolayers, AFM images, the plots of the current as a function of scan rate; plot of ratio of anodic to cathodic current as a function of scan rate ($\nu$), and the UV−vis spectrum of the cytochrome *c* (Figure S1−S11 and Table S1). This material is available free of charge *via* the Internet at http://pubs.acs.org.

## REFERENCES AND NOTES

1. Chidsey, C. E. D.; Loiacono, D. N. Chemical Functionality in Self-Assembled Monolayers: Structural and Electrochemical Properties. *Langmuir* **1990**, *6*, 682–691.
2. Uosaki, K.; Sato, Y.; Kita, H. Electrochemical Characteristics of a Gold Electrode Modified with a Self-Assembled Monolayer of Ferrocenylalkanethiols. *Langmuir* **1991**, *7*, 1510–1514.
3. Waldeck, D. H.; Khoshtariya, D. E. Fundamental Studies of Long- and Short-Range Electron Exchange Mechanisms between Electrodes and Proteins. In *Applications of Electrochemistry and Nanotechnology in Biology and Medicine I*; Eliaz, N., Ed.; Modern Aspects of Electrochemistry 52; Springer: New York, 2011; pp 105−238.
4. Naaman, R.; Waldeck, D. H. The Chiral Induced Spin Selectivity Effect. *J. Phys. Chem. Lett.* **2012**, *3*, 2178–2187.
5. Naaman, R.; Waldeck, D. H. *Supramolecular Materials for Opto-Electronics*; RSC: Oxfordshire, U.K., 2015; Chapter-6.
6. Aogaki, R.; Fueki, K.; Mukaibo, T. Application of Magnetohydrodynamic Effect to the Analysis of Electrochemical Reactions-1. MHD Flow of an Electrolyte Solution in an Electrode-Cell with a Short Rectangular Channel. *Denki Kagaku* **1975**, *43*, 504–508.
7. Fahidy, T. Z. Magnetoelectrolysis. *J. Appl. Electrochem.* **1983**, *13*, 553–563.
8. Mogi, I. *New Challenges in Organic Electrochemistry*; Gordon and Breach Science Publishers: Amsterdam, The Netherlands, 1998; Chapter 1.
9. Alemany, A.; Chopart, J.-P. *Magnetohydrodynamics*; Springer: Dordrecht, The Netherlands, 2007; Part IV.
10. Diao, Z.; Dunne, P. A.; Zangari, G.; Coey, J. M. D. Electrochemical Noise Analysis of the Effects of a Magnetic Field on Cathodic Hydrogen Evolution. *Electrochem. Commun.* **2009**, *11*, 740–743.
11. Iida, T.; Matsushima, H.; Fukunaka, Y. Water Electrolysis under a Magnetic Field. *J. Electrochem. Soc.* **2007**, *154*, E112–E115.
12. Lin, M.-Y.; Hourng, L.-W. Effects of Magnetic Field and Pulse Potential on Hydrogen Production *via* Water Electrolysis. *Int. J. Energy Res.* **2014**, *38*, 106–116.
13. Monzon, L. M. A.; Coey, J. M. D. Magnetic Fields in Electrochemistry: The Lorentz Force. A Mini-Review. *Electrochem. Commun.* **2014**, *42*, 38–41.
14. Monzon, L. M. A.; Coey, J. M. D. Magnetic Fields in Electrochemistry: The Kelvin Force. A Mini-Review. *Electrochem. Commun.* **2014**, *42*, 42–45.
15. Pullins, M. D.; Grant, K. M.; White, H. S. Microscale Confinement of Paramagnetic Molecules in Magentic Field Gradients Surrounding Ferromagnetic Microelectrodes. *J. Phys. Chem. B* **2001**, *105*, 8989–8994.
16. Ueno, S. *Biological Effects of Magnetic and Electromagnetic Fields*; Plenum Press; New York, NY, 1996.
17. McCann, J.; Dietrich, F.; Rafferty, C.; Martin, A. O. A Critical Review of the Genotoxic Potential of Electric and Magnetic Fields. *Mutat. Res.* **1993**, *297*, 61–95.
18. Walker, M. M.; Diebel, C. E.; Haugh, C. V.; Pankhurst, P. M.; Montgomery, J. C.; Green, C. R. Structure and Function of the Vertebrate Magnetic Sense. *Nature* **1997**, *390*, 371–376.
19. Phirke, P. S.; Kubde, A. B.; Umbarkar, S. P. The Influence of Magnetic Field on Plant Growth. *Seed Sci. Technol.* **1996**, *24*, 375–392.
20. Katz, E.; Lioubashevski, O.; Willner, I. Magnetic Field Effects on Cytochrome c-Mediated Bioelectrocatalytic Transformations. *J. Am. Chem. Soc.* **2004**, *126*, 11088–11092.
21. Scott, A. M.; Miura, T.; Ricks, A. B.; Xance, Z. E. X.; Giacobbe, E. M.; Colvin, M. T.; Wasielewski, M. R. Spin-Selective Charge Transport Pathways through p-Oligophenylene-Linked Donor-Bridge-Acceptor Molecules. *J. Am. Chem. Soc.* **2009**, *131*, 17655–17666.
22. Wasielewski, M. R. Energy, Charge and Spin Transport in Molecules and Self-Assembled Nanostructures Inspired by Photosynthesis. *J. Org. Chem.* **2006**, *71*, 5051–5066.
23. Verhoeven, J. W. On the Role of Spin Correlation in the Formation, Decay, and Detection of Long-lived, Intramolecular Charge-transfer States. *J. Photochem. Photobiol., C* **2006**, *7*, 40–60.
24. Lyons, M. E. G.; O'Brien, R.; Kinsella, M.; Mac Gloinn, C.; Scully, P. N. Magnetic Field Effects in Ferrocenealkane

Thiol Self Assembled Monolayer Modified Electrodes. *Int. J. Electrochem. Sci.* **2010**, *5*, 1310–1341.
25. Lyons, M. E. G.; O'Brien, R.; Kinsella, M.; Mac Gloinn, C.; Keeley, G. P.; Scully, P. N. Effect of External Magnetic Fields on Electron Transfer and Ion Pairing Dynamics at Ferrocenyl Alkane Thiol SAM/Solution Interfaces. *Electrochem. Commun.* **2010**, *12*, 1527–1530.
26. Lee, C.-C; Chou, T.-C. Effects of Magnetic Field on the Reaction Kinetics of Electroless Nickel Deposition. *Electrochim. Acta* **1995**, *40*, 965–970.
27. Devos, O.; Aaboubi, O.; Chopart, J.-P.; Oliovier, A.; Gabrielli, C.; Tribollet, B. Is There a Magnetic Field Effect on Electrochemical Kinetics? *J. Phys. Chem. A* **2000**, *104*, 1544–1548.
28. Lyons, M. E. G.; O'Brien, R.; Kinsella, M.; Mac Gloinn, C.; Scully, P. N. Magnetic Field Effects in Ferrocenealkane Thiol Self Assembled Monolayer Modified Electrodes. *Int. J. Electrochem. Sci.* **2010**, *5*, 1310–1341.
29. Lyons, M. E. G.; O'Brien, R.; Kinsella, M.; Mac Gloinn, C.; Keeley, G. P.; Scully, P. N. Effect of External Magnetic Fields on Electron Transfer and Ion Pairing Dynamics at Ferrocenyl Alkane Thiol SAM/Solution Interfaces. *Electrochem. Commun.* **2010**, *12*, 1527–1530.
30. Saravanan, G.; Ozeki, S. Magnetic Field Control of Electron Tunneling Pathways in the Monolayer of (Ferrocenylmethyl)dodecyldimethylammonium Bromide on a Gold Electrode. *J. Phys. Chem. B* **2008**, *112*, 3–6.
31. Mogi, I.; Watanabe, K. Chiral Electrode Behavior of Magneto-Electrodeposited Cu-$Cu_2O$ Films. *J. Phys.: Conf. Ser.* **2009**, *156*, 012027.
32. Mogi, I.; Watanabe, K. Enantioselective Recognition of Tartaric Acid on Magneto-electrodeposited Copper Film Electrodes. *Chem. Lett.* **2012**, *41*, 1439–1441.
33. Trojanowicz, M. Enantioselective Electrochemical Sensors and Biosensors: A Mini-Review. *Electrochem. Commun.* **2014**, *38*, 47–52.
34. Challier, L.; Mavré, F.; Moreau, J.; Fave, C.; Schöllhorn, B.; Marchal, D.; Peyrin, E.; Noël, V.; Limoges, B. Simple and Highly Enantioselective Electrochemical Aptamer-Based Binding Assay for Trace Detection of Chiral Compounds. *Anal. Chem.* **2012**, *84*, 5415–5420.
35. Granot, E.; Tel-Vered, R.; Lioubashevski, O.; Willner, I. Stereoselective and Enantioselective Electrochemical Sensing of Monosaccharides Using Imprinted Boronic Acid-Functionalized Polyphenol Films. *Adv. Funct. Mater.* **2008**, *18*, 478–484.
36. Ohno, Y.; Young, D. K.; Beschoten, B.; Matsukura, F.; Ohno, H.; Awschalom, D. D. Electrical Spin Injection in a Ferromagnetic Semiconductor Heterostructure. *Nature* **1999**, *402*, 790–792.
37. Mishra, D.; Markus, T. Z.; Naaman, R.; Kettner, M.; Göhler, B.; Zacharias, H.; Friedman, N.; Sheves, M.; Fontanesi, C. Spin-Dependent Electron Transmission through Bacteriorhodopsin Embedded in Purple Membrane. *Proc. Natl. Acad. Sci. U.S.A.* **2013**, *110*, 14872–14876.
38. Dressler, D. H.; Mastai, Y. Chiral Crystallization of Glutamic Acid on Self Assembled Films of Cysteine. *Chirality* **2007**, *19*, 358–365.
39. Ju, H.; Xiao, Y.; Lu, X.; Chen, H. Electrooxidative Coupling of a Toluidine Blue O Terminated Self-Assembled Monolayer Studied by Electrochemistry and Surface Enhanced Raman Spectroscopy. *J. Electroanal. Chem.* **2002**, *518*, 123–130.
40. Moodera, J. S.; Mathon, G. *J.* Spin Polarized Tunneling in Ferromagnetic Junctions. *Magn. Magn. Mat* **1999**, *200*, 248–273.
41. Eib, W.; Alvarado, S. F. Spin-Polarized Photoelectrons from Nickel Single Crystals. *Phys. Rev. Lett.* **1976**, *37*, 444–446.
42. Tarlov, M. J. Electron-Transfer Reaction of Cytochrome c Adsorbed on Carboxylic Acid Terminated Alkanethiol Monolayer Electrodes. *J. Am. Chem. Soc.* **1991**, *113*, 1847–1849.
43. Einati, H.; Mishra, D.; Friedman, N.; Sheves, M.; Naaman, R. Light-controlled Spin Filtering in Bacteriorhodopsin. *Nano Lett.* **2015**, *15*, 1052–1056.
44. Carmeli, I.; Skakalova, V.; Naaman, R.; Vager, Z. Magnetization of Chiral Monolayers of Polypeptide—A Possible Source of Magnetism in Some Biological Membranes. *Angew. Chem.; Int. Ed.* **2002**, *41*, 761–764.
45. Kettner, M.; Göhler, B.; Zacharias, H.; Mishra, D.; Kiran, V.; Naaman, R.; Fontanesi, C.; Waldeck, D. H.; Sęk, S.; Pawłowski, J.; Juhaniewicz, J. Spin Filtering in Electron Transport through Chiral Oligopeptides. *J. Phys. Chem. C* **2015**, 10.1021/jp509974z.
46. Cottrell, F. G. Residual Current in Galvanic Polarization Regarded as a Diffusion Problem. *Z. Phys. Chem.* **1903**, *42*, 385–431.
47. Bard, A. J.; Faulkner, L. R. *Electrochemical Methods. Fundamentals and Applications*; 2nd ed.; John Wiley & Sons: New York, NY, 2001.